Provided for non-commercial research and education use.
Not for reproduction, distribution or commercial use.

VOLUME 43 NUMBER 2 FEBRUARY 2008 ISSN 0749-6036

Superlattices and Microstructures

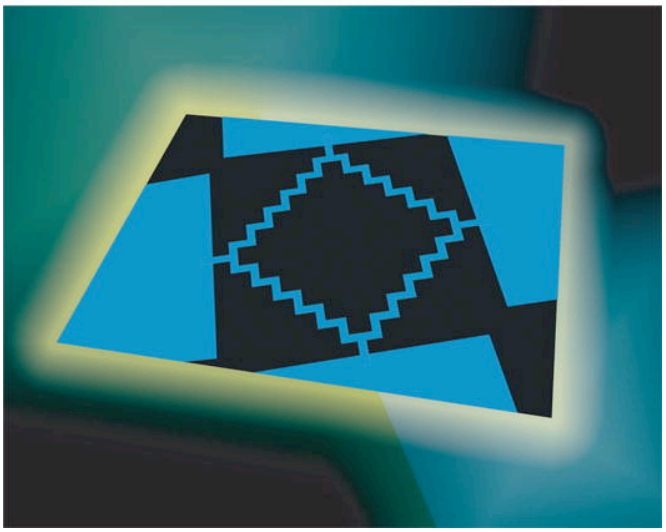

This article was published in an Elsevier journal. The attached copy is furnished to the author for non-commercial research and education use, including for instruction at the author's institution, sharing with colleagues and providing to institution administration.

Other uses, including reproduction and distribution, or selling or licensing copies, or posting to personal, institutional or third party websites are prohibited.

In most cases authors are permitted to post their version of the article (e.g. in Word or Tex form) to their personal website or institutional repository. Authors requiring further information regarding Elsevier's archiving and manuscript policies are encouraged to visit:

http://www.elsevier.com/copyright

Author's personal copy

Available online at www.sciencedirect.com
ScienceDirect
Superlattices and Microstructures 43 (2008) 101–111
Superlattices and Microstructures
www.elsevier.com/locate/superlattices

Temperature dependence of the magnetic interlayer ordering in Fe(3)/V(14)H_x (001) superlattices

B. Hjörvarsson[a,*], G. Andersson[a], J.A. Dura[b], T.J. Udovic[b], P. Isberg[c], C.F. Majkrzak[b]

[a] *Uppsala University, Department of Physics, Box 530, SE-751 21 Uppsala, Sweden*
[b] *NIST Center for Neutron Research, National Institute of Standards and Technology, MS 8562, Gaithersburg, MD 20899-8562, USA*
[c] *ABB Corporate Research, SE-721 28 Västerås, Sweden*

Received 22 November 2006; received in revised form 30 June 2007; accepted 22 July 2007
Available online 4 September 2007

Abstract

The magnetic interlayer ordering in Fe(3)/V(14)H_x (001) superlattices exhibits dramatic changes on changing the hydrogen concentration. From initial antiferromagnetic (AF) coupling with $T_N = 370(7)$ K, the introduction of H (H/V atomic ratio of 0.06) gives rise to ferromagnetic (FM) alignment at room temperature. When cooled, the magnetic ordering exhibits a transition from FM to a canted state below 200 K. Further increase of the hydrogen content (H/V $\approx$ 1) gives rise to FM-ordering at temperatures between 30 and 300 K.
© 2007 Elsevier Ltd. All rights reserved.

Keywords: Superlattice; Magnetic coupling; Magnetic ordering; Neutron reflectivity

1. Introduction

Since the discovery of the oscillatory magnetic ordering in metallic multilayers [2,3], substantial work has been devoted to the exploration of the exchange coupling. Currently, the RKKY [4] and the quantum-well [5] models are the commonly accepted interpretations for

* Corresponding author. Tel.: +46 184713837; fax: +46 184713524.
E-mail address: Bjorgvin.Hjorvarsson@fysik.uu.se (B. Hjörvarsson).

0749-6036/$ - see front matter © 2007 Elsevier Ltd. All rights reserved.
doi:10.1016/j.spmi.2007.07.030

Author's personal copy

the coupling in transition metals. Both these models attribute the basis of the coupling to extremal values of the Fermi wavevector and the discrete lattice spacing of the constituents. In both, the coupling between ferromagnetic (FM) layers oscillates between parallel (*i.e.*, FM) and antiparallel (*i.e.*, antiferromagnetic, AFM) alignments as a function of the thickness of an intervening spacer layer. Biquadratic coupling (BQ) is not obtained as an intrinsic property within these theories. Models such as that presented by Slonczewski [6] are required to describe the occurrence of BQ-ordering. The bases of his models are the existence of "loose spins" at the interfaces or competing FM and AFM interactions originating from the discrete variation in the thickness of the spacer layers.

The interlayer exchange coupling in multilayers can be tuned by, for example, alloying the spacer layer. By alloying, it is possible to shift the AFM region, as well as the strength of the coupling. When the spacer layer does absorb hydrogen exothermically and the magnetic layer does not, it is possible to selectively *"alloy"* the spacer layer *after growth*. Hence, by alloying with hydrogen, it should be possible to strongly influence the exchange coupling of magnetic heterostructures. The plausibility of this experimental route has been demonstrated for two types of multilayers, namely Fe/Nb(110) and Fe/V(001) [7–10], where Nb and V absorb hydrogen exothermally and Fe does not.

The hydrogen uptake of Fe/V superlattices is well-known; see, e.g., Ref. [11] and references therein. Fe/V samples can be reversibly loaded and unloaded with hydrogen at room temperature, or higher, without their structural quality being affected. Concentrations close to 1 in H/V (atomic ratio) are reversibly obtained, in remarkable contrast to, e.g., the previously observed cycling effects in Nb (110) films [12]. The introduction of hydrogen allows one, therefore, to alter the electronic structure of the spacer layer, without affecting the interface roughness or the intermixing of the sample. In Fe(3)/V(15) and Fe(3)/V(16) superlattices, where the numbers in the brackets denote the number of monolayers, the introduction of H was found to induce an AFM-ordering in a narrow H concentration range [9,10]. It was concluded that the transition could not be caused by the change in V thickness, since this would require contraction of the V layers. The modification of the Fermi surface in the V layers must therefore be responsible for the observed changes in the magnetic ordering.

The influence of hydrogen on the exchange coupling was explored theoretically by Ostanin et al. [13]. Their analysis supported the view of the importance of the changes in the electronic structure, as compared to the changes in the lattice parameter. Furthermore, the magnetic moment of the Fe interface layers was influenced by the presence of hydrogen in V, through the Fe–V hybridization, at the interfaces. The moment of the V interface layer (AF alignment with respect to Fe) was less affected by the presence of H, according to [13]. The change in the total moment was recently determined by in situ measurements [14], for 2, 3 and 6 monolayers of Fe in Fe/V superlattices. The results unambiguously proved a large increase of the macroscopic moment and an increased ordering temperature for these structures at high hydrogen concentrations. Thus the experimental and the theoretical investigations are consistent with respect to the reduction of the Fe-magnetic moment at the interfaces, the cause being the hybridization with V. By introducing H in the V layers, the hybridization is affected, causing an increase in the moment of the Fe layers. However, no conclusive evidence on the balance between the changes of the moment in V and Fe exists.

Here we will explore the temperature dependence of the magnetic ordering in an Fe(3)/V(14)H_x (001) superlattice (with $x = 0$, 0.06 and 1). We will show non-trivial temperature dependence, including a transition from an FM to a canted state. The origin of these changes will be discussed within the current theoretical understanding of these structures.

Author's personal copy

2. Experimental details

2.1. Sample preparation

The Fe/V (001) superlattice was grown on $20 \times 20 \times 1$ mm^3 epi-MgO (001) substrates, as described in Ref. [15]. There were 70 double layers (3 ML Fe and 14 ML V) with a total thickness of 178 nm. The sample was covered with 10 nm Pd to prevent oxidation and to facilitate hydrogen uptake and release. X-ray reflectivity and high-angle X-ray diffraction analysis revealed good crystal quality, well-defined repeat length, and chemically sharp interfaces. The layers have an intrinsic ± 1 monolayer thickness variation, as the growth is not phase locked. The thickness variation originates from the incomplete formation of the last monolayer of each layer during the growth. The Fe/V superlattice is oriented with the [100] and [010] directions along the substrate diagonals [14].

2.2. Neutron scattering

The magnetic interlayer ordering can be directly monitored using spin-polarized neutron reflectivity [16–18]; thus the chemical composition and the vectorial magnetization profile in the sample can, in principle, be simultaneously determined. The measurements were performed with neutron wavelength 0.475 nm on the NG1 Reflectometer at the NIST Center for Neutron Research, in air and in a closed cycle cryostat with in situ H-loading capabilities. A similar instrument has been described in the literature [1]. The sample was mounted so that the magnetic field was applied along the Fe/V [110] direction, which is parallel to the MgO substrate edge. Measurements were made between 30 and 350 K in a field between 8 and 2000 G. The hydrogen pressure was varied from 0.1 to 10^5 Pa. The kinetics were sufficiently fast enough to allow one to load and unload the samples at room temperature.

The incident neutrons can be polarized in one of two states, $+$ or $-$, and can be scattered with or without change of state. Thus four cross sections, $(+, +)$, $(+, -)$, $(-, +)$, and $(-, -)$ can be measured, where the first and second signs refer to the incident and scattered polarization states, respectively. The non-spin-flip (NSF) scattering is due to a combination of the chemical scalar scattering potential (n) and the component of the magnetic moment vector perpendicular to the momentum transfer vector, $\boldsymbol{Q}$, and along the polarization axis (y) which is parallel to the applied field. The $(+, +)$ scattering depends on the sum of these potentials, whereas the $(-, -)$ scattering depends on their difference. For a superlattice structure, the first peak in the scattered intensity will be found at scattering vector $Q_1 = 2\pi/\Lambda$ corresponding to the superlattice repeat distance, Λ. A ferromagnetic contribution of the Fe layers can be derived from the splitting between the $(+, +)$ and $(-, -)$ cross sections at the Q_1 peak position. The splitting is, to a first approximation, proportional to the product of the projection of the magnetic moment (m_y) and the contrast in nuclear scattering length ($\Delta n = n_{\mathrm{Fe}} - n_{\mathrm{VH}}$), ($I_{(+,+)} - I_{(-,-)} \propto \Delta n \cdot m_y$). Hence, a change in hydrogen concentration and projection of the magnetic moment will affect the splitting. For the present sample structure, the nuclear contrast increases with increasing hydrogen content.

The spin-flip scattering (SF) arises from the component of the in-plane magnetization perpendicular to the polarization axis. At $Q_{1/2} = 1/2 Q_1$, a peak in the scattered intensity would correspond to a magnetic structure with twice the period of the chemical modulation, e.g., an AFM or canted state structure. The degree of AFM-order can be deduced from the SF scattering into the half-order peaks, $Q_{1/2}$. The intensity of the SF scattering scales as the projection in the direction of the beam of magnetic scattering amplitude squared $\left(I_{(+,-)} = I_{(-,+)} \propto m_x^2\right)$. Hence,

Author's personal copy

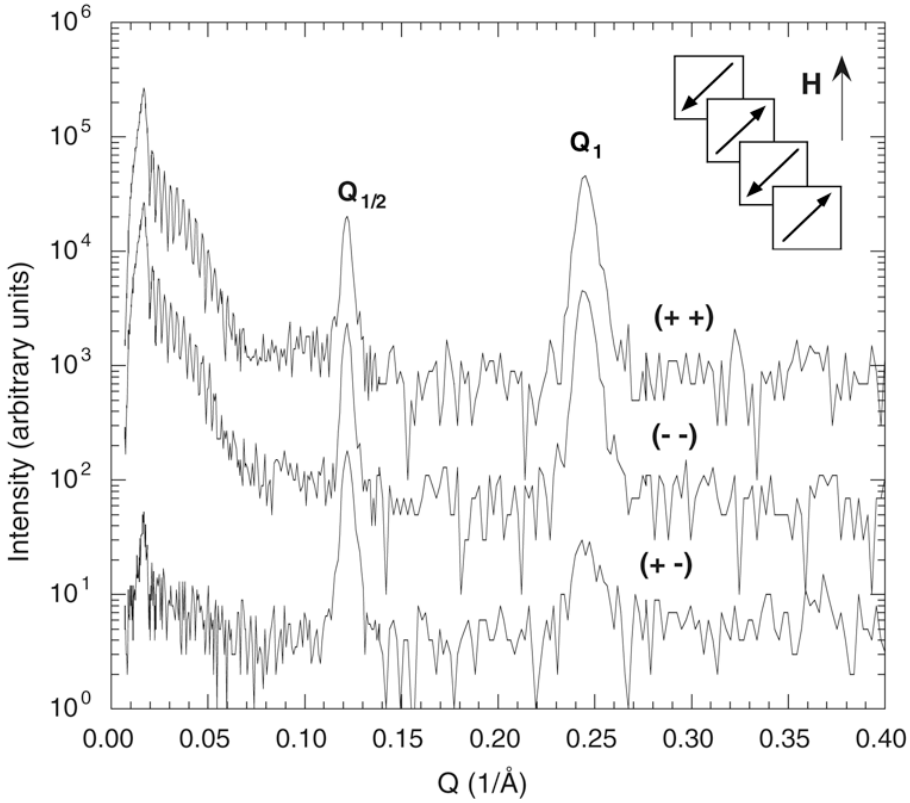

Fig. 1. Reflectivity data from the hydrogen-free sample at 30 K, with an applied field of 25 G along the [110] axis. The uppermost curve is the non-spin-flip (+, +), the middle curve is the (−, −) and the bottom one is the (+, −) data. The magnetic structure of the sample is indicated in the insert: the magnetic moments of the layers are rotated 45° with respect to the applied field.

by combining the different components from the spin-flip and the non-spin-flip intensities, a full in-plane configuration of the magnetic moments of the layers can be obtained.

3. Results and discussion

3.1. Hydrogen-free sample

The accessible range in magnetic field is strongly limited when using the low-temperature sample stage. Therefore, a number of scans were performed at ambient temperature, to determine the details of the initial magnetic state of the sample. A typical reflectivity curve is shown in Fig. 1. For clarity we only display the (+, +), (−, −) and the combined spin-flip components, since (+, −) and (−, +) are identical. As seen in the figure, a number of rapid oscillations are present at low Q values. These oscillations originate from the interference of neutrons scattered at the back and the front side of the superlattice sample. Hence, the variation in the total thickness is small. The magnetic profile in Fe/V(001) superlattices has been discussed in experimental [19,20] as well as theoretical [21,22] works as described in the literature. Although some inconsistency on the details exists, all these support a reduction of the Fe moment at the Fe/V interfaces. Furthermore, the proximity to Fe causes a magnetization of the V interface layers [19–21]. The V moment is aligned antiferromagnetically with respect to the Fe moment.

A number of scans (around $Q_{1/2}$ and Q_1) were performed at fields up to 2000 G at room temperature. In the range of 50–1000 G, the difference in the NSF intensity ($I_{(+,+)}-I_{(-,-)} \propto$

Author's personal copy

$\Delta n \cdot m_y$) at Q_1 scaled nearly linearly with the field. In the same field range, the square root of the half-order SF intensity scaled as $\left[1-(H/H_0)^2\right]$, as expected for AFM-interlayer-coupled samples. The saturation field (H_0) was determined to be 1.1 (1) kG at 300 K from these measurements. The presence of a V-magnetic moment at the interface does not influence this analysis, since we are regarding the first-order Fourier component of the scattering profile, which is determined by the difference in scattering length density (b) and not the detailed shape of the magnetic profile.

In the range 0–50 G, large changes in the SF, as well as the NSF intensities were observed. At 25 G (see Fig. 1), the SF and the NSF components have approximately the same intensity at $Q_{1/2}$. This is consistent with both in-plane components of the magnetization being aligned antiparallel in alternating layers, with roughly equal components of alternating moment along the x and y axes. At fields larger than 45 G, no NSF component is observed at $Q_{1/2}$.

Hence, the data are consistent with a reorientation of the magnetic moment. At low fields, the moments of the AF coupled sample are tilted $\pi/4(3\pi/4)$, with respect to the applied field. With increasing field, the moments are rotated, and are close to $\pm\pi/2$ at around 45 G. Hence, the results are consistent with an AFM structure, with weak anisotropy and the easy axes being (100) and (010).

Simulations of data, using the polarized reflectometry analysis code at NIST confirmed the consistency of the deduced magnetic ordering. From these measurements, the anisotropy field was determined to be 45 ± 5 G at room temperature. Hence both the field dependence and the detailed simulations of the scattering profile were consistent with the magnetic moments of the Fe being aligned in the (100) and ($\bar{1}00$) or (010) and ($0\bar{1}0$) directions, *i.e.*, two of the easy axes of magnetization. The deduced magnetic ordering is indicated in an inset in Fig. 1.

At 300 K, samples with exactly 3 monolayers of Fe are found to be magnetically isotropic in the plane, independent of the V layer thickness. However, the anisotropy appears and increases with increasing Fe thickness [23]. Hence the average thickness of the Fe layers in the current sample can be inferred to be slightly larger than 3 monolayers.

The influence of the temperature on the magnetic ordering is illustrated in Fig. 2, where the reduced magnetic moment ($m = M/M_S$) of the layers, is plotted as a function of temperature. The measurements were performed with an external field of 100 G, which is roughly two times larger than the anisotropy field at room temperature. Consequently, a reorientation of the magnetic moments is observed at a temperature where the anisotropy field becomes larger than the applied field. This transition takes place between 250 and 300 K, as indicated in the figure. The magnetic ordering, with respect to the applied field, is also illustrated in the figure. By fitting the reduced moment with $(1 - T/T_N)^\beta$, an ordering temperature (Néel temperature, T_N) of 370 ± 7 K is obtained with an effective exponent $\beta = 0.34 \pm 0.03$. The resulting fitting is shown as a dotted curve in the figure.

The deduced magnetic ordering was compared to results from a calculation using a phenomenological model, described in Refs. [23,24]. In short, the energy density of a magnetic bilayer with four-fold in-plane anisotropy is given by

$$E = -\frac{J_1}{d}\cos(\theta_1-\theta_2) + \frac{J_2}{d}\cos^2(\theta_1-\theta_2) + \frac{1}{2}\frac{K}{4}\left(\sin^2 2\theta_1 + \sin^2 2\theta_2\right) - \frac{Hm}{2}\left(\cos(\theta_1-\phi)+\cos(\theta_2-\phi)\right) \quad (1)$$

where J_1 is the bilinear coupling constant, J_2 is the biquadratic coupling constant, θ_i is the angle of the magnetization m in layer i with respect to the easy axis, K is the anisotropy and

Author's personal copy

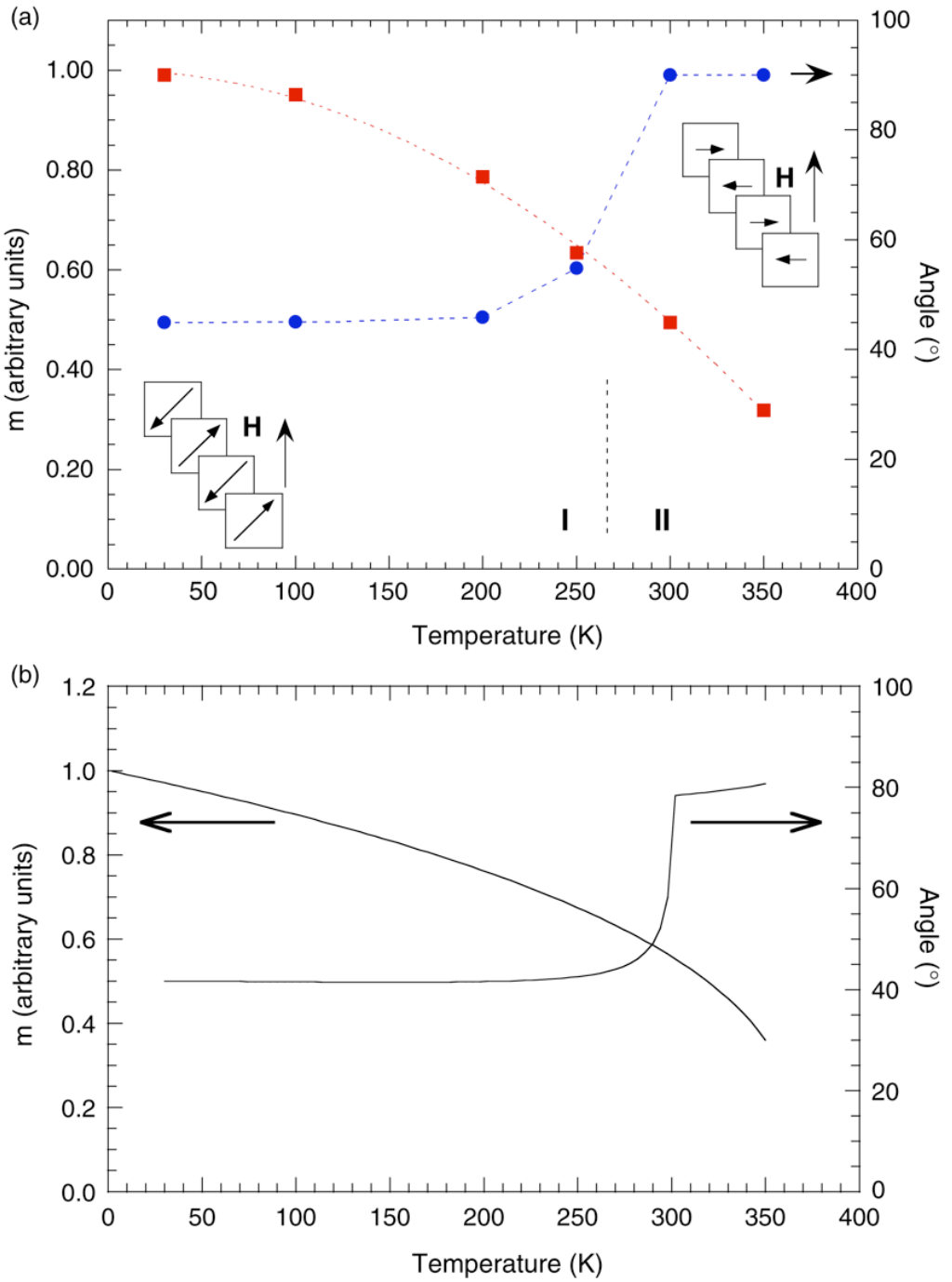

Fig. 2. (a) The temperature dependence of the reduced magnetic moment of the layers in the AFM structure. The in-plane rotation of the moment is included and illustrated as an insert in the figure. The applied field is 100 G along the [110] axis. The regions marked in the figure correspond to the different anisotropy regions. (I) The anisotropy locks the AFM ordered moments in the direction of the easy axis. (II) The moments are perpendicular to the applied field. (b) The simulated temperature dependence of the reduced magnetic moment and the angle of the layers with respect to the magnetic field. For details, see text.

ϕ is the angle between the easy axis and the applied field H. The magnetization was assumed to be the same for all the Fe layers. By minimizing the energy with respect to the angles θ_i, the projection of the magnetic moment on any axis is easily obtained. The projected moment and the angle between the applied field and one of the Fe layers were modeled using Eq. (1)

Author's personal copy

and the results are shown in Fig. 2(b). The bilinear and biquadratic coupling constants were set to be $J_1\{\mathrm{J/m^2}\} = -\mathrm{H}_s\mathrm{M}_s d_{\mathrm{Fe}}/4$ and $J_2 = 0$. As seen in the figure, the experimental data in Fig. 2(a) are qualitatively as well as quantitatively reproduced. The saturation field was previously determined to be linear with temperature, $\mathrm{H}_s\{\mathrm{T}\} = 0.306–0.2 \times 10^{-3} T\ \{\mathrm{K}\}$, in Fe(3)/V(14) superlattices [25]. Furthermore, the anisotropy was previously established to be linear with temperature for Fe(4)/V(4) samples [26]. As seen in the figure, a linear model ($K\ \{\mathrm{J/m^3}\} = 13\,650–43.5\ \mathrm{T}\{\mathrm{K}\}$) seems to be sufficient to describe the changes in the anisotropy.

3.2. Low hydrogen content

When a small amount of hydrogen is introduced in the sample at room temperature, a transition from AFM- to FM-ordering is obtained. At a relative change in the scattering vector of the superlattice peak, $\Delta Q_1/Q_1 = 0.02$, full FM-ordering is achieved. The structural change corresponds to an average hydrogen concentration of 6 at. % in the V layers, using the previously inferred relation between the hydrogen concentration and expansion [27,28]. A field scan at 300 K clearly showed a remanence, consistent with FM-interlayer ordering. Substantial field dependence of the projected moment was observed (100%/100 G). In Fig. 3(a), we display the spin-flip intensity at the $Q_{1/2}$ position and the differences in the integrated intensities of the NSF peak at the Q_1 position at different temperatures. The hydrogen pressure was kept constant during these measurements. The change in $\Delta Q_1/Q_1$ with temperature corresponded to the change induced by the thermal contraction/expansion, which was determined to be $8.2(8) \times 10^{-6}\ \mathrm{K}^{-1}$ for the H-free sample. Hence, the hydrogen concentration is unaffected by the thermal cycling, presumably due to kinetic restrictions.

In order to provide consistent magnetic states as a starting point for the experiments, the data were collected in the following manner: The sample was cooled from ambient to 30 K, while a field of −320 G was applied. Thereafter the field was reversed, and increased to +51 G. After measuring the reflectivity at 30 K (51 G), the temperature was increased in steps and the reflectivity was measured at each temperature. After reaching 300 K, the measurements were repeated with decreasing temperature. The observed ordering was found to be reversible with respect to field and temperature, except in a small region close to the transition temperature, where there was a significant difference between the cooling and heating. As indicated in the figure, the Fe layers are FM-aligned above 200 K. Between 160 and 200 K the ordering is dominated by an FM contribution. However, an indication of a pre-stage to the low-temperature phase is evident from the turnover in the NSF contribution with decreasing temperature. The turnover can be the onset of the canted state, stabilized either by anisotropy or biquadratic coupling. The FM-ordering temperature is estimated to be ≈350 K, *i.e.* somewhat lower than that in the unloaded sample. The accuracy of the measurements prohibits more quantitative comparison. A slight decrease in the ordering temperature is consistent with decreased interlayer coupling, which is the opposite of the observed increase in bilinear coupling in NbH_x/Co multilayers [29]. Below 160 K, a reorientation of the moments takes place and the magnetic profile is best described as a canted state. The change in NSF intensity is consistent with a close to $\pi/4$ rotation of the moment from the direction of the magnetic field. The deduced magnetic order is depicted in insets in the figure.

The field dependence was investigated at 30 K. The maximum applied field obtained with cooling was 125 G, which is not sufficient for aligning the magnetic moments of the Fe layers. A

Author's personal copy

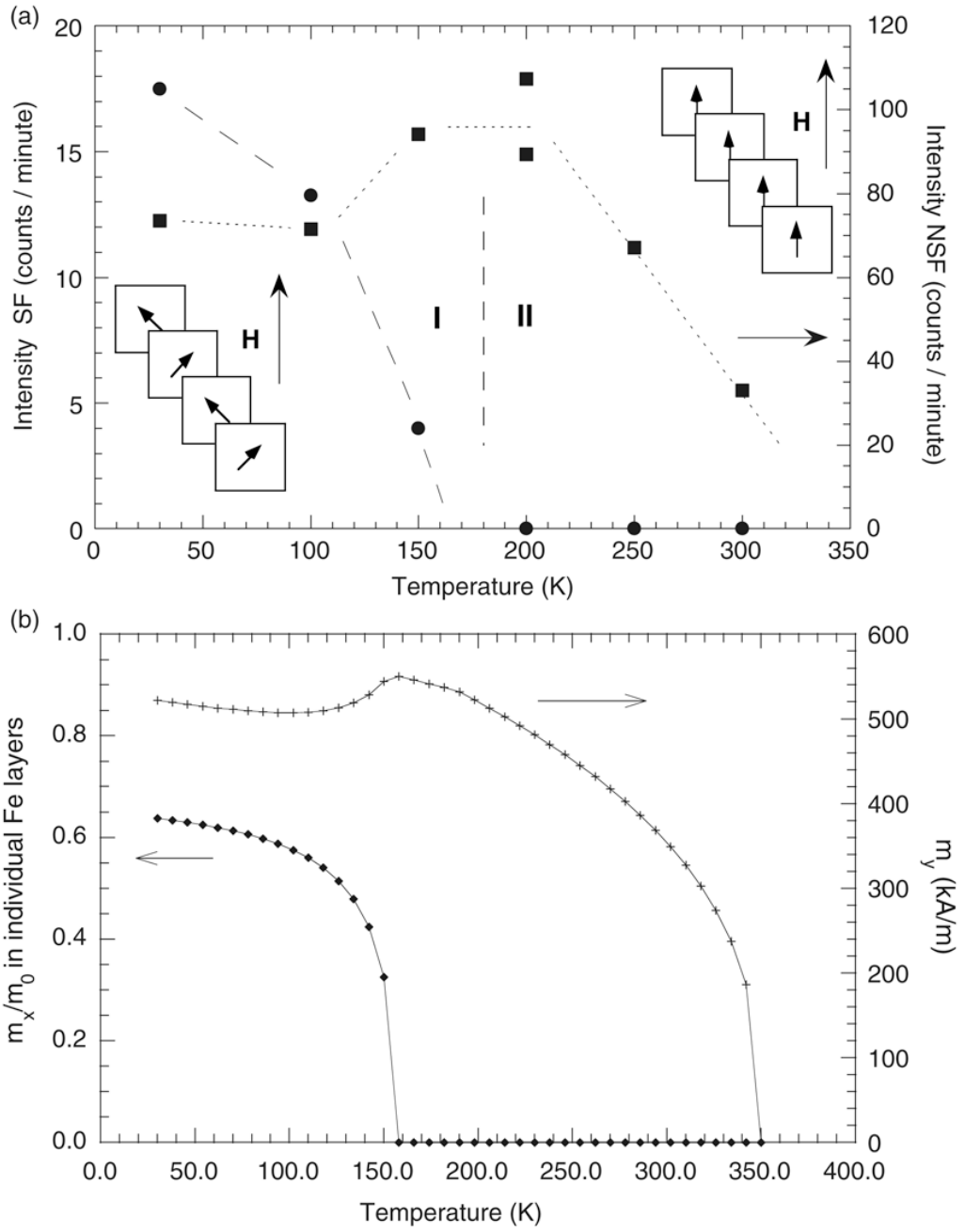

Fig. 3. (a) Half-order peak intensity of the SF and the splitting between the NSF intensities of the Q1 peaks, with an applied field of 51 G along the [110] axis. The hydrogen content of the sample is $\simeq 0.06$ (H/V atomic ratio). The statistical error is of the size of the symbols. (b) The simulated magnetic interlayer ordering in the presence of H in the V layers with the anisotropy K reduced to 25% of the value used for the hydrogen-free sample. For details, see text.

saturation field of 191 ± 6 G was obtained by extrapolation, which corresponds roughly to 1/5 of the saturation field at 300 K in the absence of hydrogen. The counting rate in the region of the $Q_{1/2}$ NSF peak was close to the background level and almost independent of the applied field. Hence, the results exclude the formation of domains with AFM- and FM-interlayer ordering, as a cause for the observed changes in the reflectivity.

Assuming that $|m_i|$ is constant at these temperatures implies a single-domain interpretation, which is in line with previous neutron analysis [8,9]. Therefore the rotation of the moment can

Author's personal copy

be obtained by using the normalized intensity of the SF component at $Q_{1/2}$. The normalization was obtained by comparing the obtained intensity of the SF component at $Q_{1/2}$ from the H-loaded sample with the corresponding intensity of the H-free sample. By extrapolating the field dependence of the intensity at 30 K to zero field, an angle close to $\pi/2$ was obtained between the adjacent layers. Increase in field or temperature decreases the angle, as expected for a canted state (BQ-ordering).

These experimental observations were used as input parameters for a simulation of the projected moment, using the model described by Eq. (1) above. The temperature dependence of the intrinsic magnetic moment in each layer was assumed to follow the previously measured asymptotic behavior. The intralayer coupling and the anisotropy were previously found to be independent of the hydrogen loading at room temperature [23], which was taken as a starting point in the simulations. However, the data were inconsistent with the latter of these assumptions. The reorientation of the interlayer order was qualitatively reproduced only with a reduction of the anisotropy by a factor of $1/2$ or less, as compared to the H-free sample. The reduction of the FM contribution around 150 K was still underestimated when the anisotropy was reduced to $1/4$ of the value used in the hydrogen-free case. The bilinear coupling constant, J_1, was set to zero in this simulation, and the biquadratic coupling was $J_2 = 1.5\mathrm{H_s}\mathrm{M_s}d_{\mathrm{Fe}}/4$. Here the saturation field was $\mathrm{H}_s\{\mathrm{T}\} = 0.052\text{–}0.34 \times 10^{-3}T\,\{\mathrm{K}\}$.

The average Fe moment does increase with H content in the V layers through the Fe–V hybridization at the interfaces [14]. It is therefore conceivable that the anisotropy as well as the ordering temperature is affected by the presence of H. The change in magnetic moment is expected to be restricted to the interface Fe layer, and the influence on the moment is expected to be minute as the change of the hydrogen content is small. It is therefore reasonable to ignore these changes and focus on the exchange coupling.

The origin of the BQ coupling (canted state) is either intrinsic or induced by steps or loose spins at the interfaces [6]. It is therefore of interest to note that the step density at the interfaces, and the amount of loose spins in the V layers cannot be altered by the introduction of H in the sample. However, the strength of the interlayer coupling is influenced by the presence of hydrogen. As a consequence, the balance between the bilinear and the biquadratic coupling strengths can be affected. By increasing the hydrogen content, the relative strength of the AFM coupling is decreased, but the introduction of 6 at. % of H is just barely enough to switch the magnetic ordering from the AFM to the FM state. Therefore, when the sample is cooled, it is plausible that there are two contributions to the rotation of the moments, *i.e.* the biquadratic coupling and the anisotropy. The moments initially rotate infinitesimally from the orientation of the field, driven by the exchange coupling, but the angle between the adjacent layers gradually increases until a close to $\pi/2$ configuration is reached at the lowest temperatures. According to our analysis, the biquadratic coupling would dominate the rotation, but a stabilization of the moment at $\pm\pi/4$ with respect to the field can be caused by the anisotropy.

An alternative understanding can be based on the ordering of local elastic dipoles in the V layers. At room temperature, the polarized local strain field is viewed to be random in the plane of the V layers. Hence, strong fluctuations are expected when regarding the nesting vectors in different regions (nm scale) of the sample. The origin of the change in the nesting vector is the pronounced local influence of H on the electronic structure of the V host [8]. Thus, a strong disorder is present, which can give rise to both temporally as well as spatially frustrated coupling. The temporal variation originates in the (high) mobility of H. The in-plane spatial correlation between the elastic poles increases with decreasing temperature, hence the expectation value of the coupling would consequently exhibit smaller temporal fluctuations with

Author's personal copy

decreasing temperatures. There are currently no measurements available on the spatial correlation between the elastic poles and the time constant of the hopping rate has not been established.

3.3. High hydrogen content

When the hydrogen content is increased to close to saturation (interior concentration, $H/V \approx 1$), no relative reorientation of the magnetic moments is observed upon cooling. The sample remains ferromagnetic at temperatures between 30 and 300 K. However, during the thermal cycling non-recoverable changes with respect to the anisotropy were observed. The magnetic moment and the ordering temperature were, within the accuracy of the measurements, the same as the H-free sample.

4. Summary

The introduction of hydrogen in the V layers in Fe(3)/V(14) (001) superlattices induces an AFM to FM transition at room temperature. With a H/V atomic ratio of 0.06 in the V layers, the transition is completed. When the sample is cooled while keeping the H/V ratio fixed at 0.06, a transition from FM to a canted state occurs around 170 K. A precursor of the transition is seen between 200 and 170 K. The saturation field at 30 K corresponds to $1/5$ of the saturation field of the H-free AFM structure at 300 K. The anisotropy of the sample is initially weakened by the introduction of H in the V layers. The canted state is found to be partially stabilized by the, albeit weak, anisotropy of the Fe layers. The origin of the canted state can be inferred to be from the local distortion in the electronic structure of V. When the H/V ratio approaches 1, the magnetic structure remains FM at temperatures between 30 and 300 K. The results illustrate the richness of the ordering of layered magnets, richness which is only partially explored at the current stage.

Acknowledgements

The support from VR and SSF is gratefully acknowledged.

References

[1] Joseph Dura, Donald Pierce, Charles Majkrzak, Nicholas Maliszewskyj, Duncan McGillivray, Mathias Loesche, Kevin O'Donovan, Mihaela Mihailescu, Ursula Perez-Salas, David Worcester, Stephen White, AND/R: Advanced neutron diffractometer/reflectometer for investigation of thin films and multilayers for the life sciences, Rev. Sci. Instr. 77 (2006) 074301.
[2] C.F. Majkrzak, J.W. Cable, J. Kwo, M. Hong, D.B. McWhan, Y. Yafet, J.V. Waszczak, C. Vettier, Phys. Rev. Lett. 56 (1986) 2700.
[3] P. Grünberg, R. Schreiber, Y. Pang, M.B. Brodsky, H. Sowers, Phys. Rev. Lett. 57 (1986) 2442.
[4] P. Bruno, C. Chappert, Phys. Rev. Lett. 67 (1991) 1602.
[5] J.E. Ortega, F.J. Himpsel, Phys. Rev. Lett. 69 (1992) 844.
[6] J.C. Slonczewski, J. Magn. Magn. Mater. 150 (1995) 13.
[7] F. Klose, Ch. Rehm, D. Nagengast, H. Maletta, A. Weidinger, Phys. Rev. Lett. 78 (1997) 1150.
[8] B. Hjörvarsson, J.A. Dura, P. Isberg, T. Watanabe, T.J. Udovic, G. Andersson, C.F. Majkrzak, Phys. Rev. Lett. 79 (1997) 901.
[9] V. Leiner, K. Westerholt, A.M. Blixt, H. Zabel, B. Hjörvarsson, Phys. Rev. Lett. 91 (2003) 037202.
[10] M. Pärnaste, M. Marcellini, B. Hjörvarsson, J. Phys. Condens. Matter 17 (2005) L477.
[11] Stefan Olsson, Anna Maria Blixt, Björgvin Hjörvarsson, J. Phys. Condens. Matter 17 (2005) 2073.
[12] C. Rehm, H. Fritzsche, H. Maletta, F. Klose, Phys. Rev. B 59 (1999) 3142.
[13] S. Ostanin, V.M. Uzdin, C. Demangeat, J.M. Wills, M. Alouani, H. Dreyssé, Phys. Rev. B 61 (2000) 4870.
[14] D. Labergerie, K. Westerholt, H. Zabel, B. Hjörvarsson, J. Magn. Magn. Mater. 225 (2001) 373.

Author's personal copy

[15] P. Isberg, B. Hjörvarsson, R. Wäppling, E.B. Svedberg, L. Hultman, Vacuum 48 (1997) 483.
[16] C.P. Felcher, Physica B 192 (1993) 137 C.
[17] C.F. Majkrzak, Physica B 173 (1993) 75.
[18] H. Zabel, Physica B 198 (1994) 156.
[19] G.R. Harp, S.S. Parkin, W.L. O'Brien, B.P. Tonner, Phys. Rev. B 51 (1995) 3293.
[20] L.-C. Duda, P. Isberg, P.H. Andersson, P. Skytt, B. Hjörvarsson, J.-H. Guo, C. Såthe, J. Nordgren, Phys. Rev. B 55 (1997) 12914.
[21] E. Holmström, L. Bergqvist, B. Skubic, B. Hjörvarsson, L. Nordström, I. Abrikosov, P. Svedlindh, O. Eriksson, Proc. Natl. Acad. Sci. USA 101 (2004) 4742.
[22] V. Uzdin, K. Westerholt, H. Zabel, B. Hjörvarsson, Phys. Rev. B 68 (2003) 214407.
[23] P. Poulopoulos, P. Isberg, W. Platow, W. Wisny, M. Farle, B. Hjörvarsson, K. Baberschke, J. Magn. Magn. Mater. 170 (1997) 57.
[24] E.E. Fullerton, J.S. Jiang, M. Grimsditch, C.H. Sowers, S.D. Bader, Phys. Rev. B 58 (1998) 12193.
[25] P. Granberg, P. Isberg, E.B. Svedberg, B. Hjörvarsson, P. Nordblad, R. Wäppling, J. Magn. Magn. Mater. 186 (1998) 154.
[26] K. Sjögren, Uppsala University Institute of Technology Report UPTEC 96:111E, August 1996.
[27] G. Andersson, B. Hjörvarsson, P. Isberg, Phys. Rev. B 55 (1997) 1774.
[28] G. Andersson, B. Hjörvarsson, H. Zabel, Phys. Rev. B 55 (1997) 15905.
[29] R. Watts, B. Rodmacq, J. Magn. Magn. Mater. 174 (1997) 70.